Electronic transport in metal-soldered carbon-nanotube multiterminal junctions

Antonis N. Andriotis*
Institute of Electronic Structure and Laser, Foundation for Research and Technology–Hellas, P.O. Box 1527, Heraklio, Crete 71110, Greece

Madhu Menon†
Department of Physics and Astronomy and Center for Computational Sciences, University of Kentucky, Lexington, Kentucky 40506, USA
(Received 26 August 2008; revised manuscript received 7 November 2008; published 8 December 2008)

The structural and conducting properties of single-wall carbon nanotubes (SWCNs) in soldered configuration is obtained using efficient formalisms based on spin-polarized tight-binding formulation incorporating full consideration of *s*, *p*, and *d* basis sets for carbon and metal atoms. The full structural relaxation of the combined SWCN and metal system is found to be essential for realistic characterization of conductivity. Soldering appears to reduce the current as well as the Ohmic character. More importantly, for multiterminal SWCN junctions, soldering can significantly alter the rectification properties by reversing its direction.

DOI: 10.1103/PhysRevB.78.235415 PACS number(s): 61.46.−w, 73.22.−f, 71.20.Tx

I. INTRODUCTION

Single-wall carbon nanotubes (SWCN) are considered to be promising candidates for use in nanoscale electronics due to their unique structural and electrical properties. In actual device applications the SWCNs must be contacted with metallic leads. SWCN in contact with metal atoms have been found to display improved electron field-emission properties.[1–4] Furthermore, as the devices based on SWCN continue to shrink, their contact resistance plays an increasing role in their transport properties. Since it is difficult to experimentally manipulate individual nanotubes, fabricating functional devices based on atomistic metal nanostructure contacts have been challenging. The popular method of electrically contacting nanostructures is electron-beam lithography.[5] This procedure is, however, found to be difficult and time consuming. More recently, a lithography-free contacting technique has been used to solder submicron-sized contacts to nanostructures.[6] The remarkable feature of this is that the contacts are not only Ohmic, but also the resultant devices are clean and the device characteristics are consistent. They have used this method to contact graphene and investigated electronic transport. The contacts thus produced have been found to sustain large currents, thereby allowing investigations of high-bias electronic transport properties. In another work, experimentalists have succeeded in welding a single nanotube to metal surface by using a combination of platinum particle encapsulated in nanotube in contact with Cu plate.[4] In this work, nanotubes were manipulated inside a high-resolution transmission microscope (HR-TEM) combined with a nanomanipulator, and a single nanotube free-standing on a platinum surface was fabricated by nanowelding.

These remarkable experimental advances have opened up the exciting possibility of creating multiterminal nanotube junctions by soldering in a controlled way, leading to the fabrication of molecular electronic devices. In particular, the three-terminal nanotube junctions such as the *T* and *Y* junctions raise the possibility of using the devices in nanoscale transistor or amplifier applications. These are most essential devices in any current-based molecular electronic circuitry arrangements due to their use in performing logic operations, as well as in compensating for power losses due to the current flow in the system.

Theoretical calculations, although very challenging, can provide a very valuable guidance in this area. The main challenge stems from the difficulties in providing a realistic characterization of the nanotube-metal contact configuration. This is very crucial for an accurate description of the nanosoldered structures.

Most of the theoretical approaches used in the studies of the transport properties of the SWCNs in contact with metal layers (MLs) assume ideal ML-SWCN interfaces, i.e., undisturbed by their mutual interaction (contact)[7–12] and, therefore, limited in the realistic description of the conducting properties of such systems. Recently, we have investigated the transport properties of SWCNs in embedded as well as in side contact with metal leads (MLs) using theoretical simulations and demonstrated the necessity of full structural relaxation of the combined SWCN and metal system for realistic characterization of conductivity.[13]

In this work we provide the first theoretical description of the multiterminal SWCN junctions obtained by soldering individual SWCNs and also provide full current vs voltage (*I-V*) characterizations for these structures. We use the transition metal Ni as a representative soldering material. The contact geometries are obtained by structural relaxations with no symmetry constraints using molecular-dynamics (MD) simulations employing tight-binding (TB) Hamiltonian.

In Sec. II we briefly describe the formalism used in the present work.

II. FORMALISM

At the level of approximation in which no spin-flipping terms are present in the Hamiltonian of the extended molecule, the calculation of its transmission coefficient and its *I-V* curves is based on the calculation of the spin-resolved Green's function, $G^{\sigma}_{\mathrm{exmol}}(E)$ ($\sigma=\pm 1$ for spin up and spin down, respectively), defined as follows:

$$G^{\sigma}_{\text{exmol}}(E) = [E - H^{\sigma}_{\text{exmol}} - \Sigma^{\sigma}_{L}(E) - \Sigma^{\sigma}_{R}(E)]^{-1}, \quad (1)$$

where $H^{\sigma}_{\text{exmol}}$ is the spin-resolved Hamiltonian of the isolated extended molecule and Σ^{σ}_{L} and Σ^{σ}_{R} are the left (L) and right (R) self-energies, respectively, which simulate the left and right contacts of the extended molecule to the metal leads.

We use the TB Hamiltonian for performing molecular-dynamics simulations.[14] The TB representation of the Hamiltonian $H^{\sigma}_{\text{exmol}}$ consists of $N_{\text{at}}N_{\text{orb}} \times N_{\text{at}}N_{\text{orb}}$ matrices, where N_{at} is the total number of atoms making up the ML-SWCN-ML system and N_{orb} is the number of orbitals on each atom. We use $N_{\text{orb}}=4$ for carbon that includes $1s$ and $3p$ orbitals and $N_{\text{orb}}=9$ for Ni that includes $1s$, $3p$, and $5d$ orbitals. The use of all these orbitals is necessary in order to allow for the correct description of the interatomic interactions between C-C, C-Ni, and Ni-Ni atoms.[14] For the investigation of the electronic transport of the ML-SWCN systems, we use the surface Green's function matching method (SGFMM).[15] In this approach we followed Datta's formalism[7] suitably modified by implementing it in the embedding approach of Inglesfield and Fisher.[16] The same TB Hamiltonian is used both in the conductivity calculation, as well as for performing molecular-dynamics simulations for structural relaxation ensuring consistency in the calculations.

Having evaluated $G^{\sigma}_{\text{exmol}}$, the spin-resolved transmission function $T_{\sigma}(E,V_b)$ can be obtained from the following equation:[7]

$$T_{\sigma}(E,V_b) = \text{tr}[\Gamma^{\sigma}_{L} G^{\sigma}_{\text{exmol}} \Gamma^{\sigma}_{R} \{G^{\sigma}_{\text{exmol}}\}^{\dagger}], \quad (2)$$

where V_b is the bias voltage,

$$\Gamma^{\sigma}_{j}(E;V_b) = i(\Sigma^{\sigma}_{j} - \{\Sigma^{\sigma}_{j}\}^{\dagger}), \quad j = L,R, \quad (3)$$

with the self-energies as obtained using the formalism of Ref. 15.

The total transmission function $T(E)$ for the extended molecule is

$$T(E,V_b) = \sum_{\sigma} T_{\sigma}(E,V_b). \quad (4)$$

Finally, the electronic current through the extended molecule due to the applied bias V_b is obtained by utilizing the formula:[7]

$$I(V_b) = \frac{2e}{h} \int_{-\infty}^{+\infty} T(E,V_b)[f_E(\mu_L) - f_E(\mu_R)]dE, \quad (5)$$

where $\mu_i = E_F - eV_i$; $i=L,R$, where V_L and V_R are applied voltages on the left and the right metal leads, respectively, $e>0$ is the electron charge, E_F is the Fermi energy, and $f_E(\mu)$ is the Fermi distribution

$$f_E(\mu) = \frac{1}{1 + e^{(E-\mu)/k_B T}}, \quad (6)$$

where k_B is Boltzmann's constant and T is the temperature. In the following we set the bias voltage $V_b = V_L - V_R$.

In the case of a Y- or a T-type SWNCs, the above formalism is generalized as follows: We assign the subscripts i,j,k to each of the three SWCN branches and let i,j represent the open edges of a two-branched SWCN. The effect of the third terminal k is incorporated in the Hamiltonian of the system by an additional self-energy term, $\Sigma^{\sigma}_{k}(E)$, which is added as an extra term within the brackets of the right-hand side of Eq. (1). For any of the (i,j) pairs of the three-terminal SWCN, the above formalism is then applied in order to define the transmission function, $T^{\sigma}_{ij}(E,V_b)$, for an electron going from branch i to branch j. Summing over the spin index we obtain the total transmission function, $T_{ij}(E,V_b)$. Having obtained all these T_{ij} functions, the current I_i in the ith branch is then given by

$$I_i(V_b) = \frac{2e}{h} \sum_{j=1}^{3} \int_{-\infty}^{+\infty} T_{ij}(E,V_b)[f_E(\mu_i) - f_E(\mu_j)]dE. \quad (7)$$

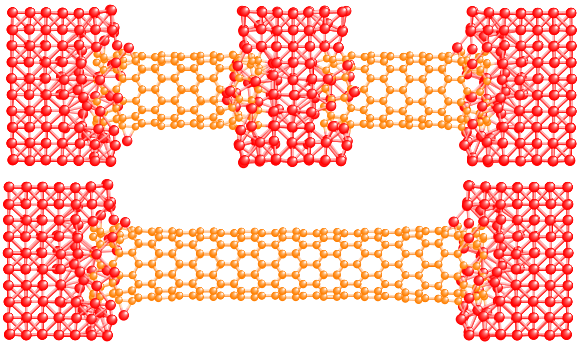

FIG. 1. (Color online) Fully relaxed geometry of two (10,0) SWCNs soldered in the middle by a Ni cluster oriented in ⟨001⟩ direction with the outer ends of each nanotube in embedded end contact with Ni surface (top panel). The bottom panel shows the relaxed nonsoldered case.

III. APPLICATIONS

We next use the formalism in Sec. II for obtaining the I-V characteristics of soldered nanotube multiterminal junctions. We consider two and three SWCNs soldered by Ni clusters with their free ends in contact with metallic leads made of Ni. Our present application includes systems in which the combined metal-SWCN systems consist of 1000–1500 atoms. These are allowed to relax through MD simulations. The soldering process is simulated by embedding open nanotube ends in Ni clusters ("embedded end-contact" configuration[13]) and by performing a full symmetry-unrestricted geometry optimization using tight-binding molecular-dynamics (TBMD) simulations.[17] The outer ends of each of the nanotubes are also in embedded end contact with Ni(001) surfaces. These Ni surfaces consist of several Ni planes and serve as MLs for contacting with the voltage sources. Following our previous work,[13] the number of Ni planes has been carefully chosen to ensure convergence of the structural relaxation of the combined metal-SWCN systems at the ends.

IV. RESULTS

In the top panel of Fig. 1 we show a relaxed structure consisting of two (10,0) SWCNs soldered in the middle by a

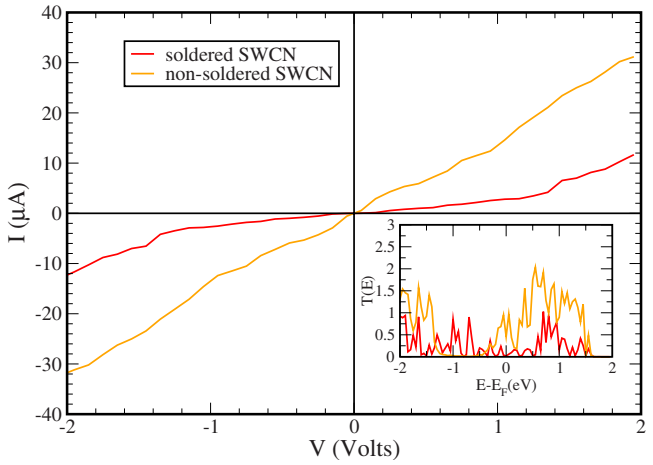

FIG. 2. (Color online) *I-V* curves for the structures in Fig. 1 for symmetric bias configurations. The transmission function, $T(E)$, for the two cases are shown in the inset.

Ni cluster oriented in ⟨001⟩ direction. The bottom panel shows the corresponding nonsoldered case. As can be seen in the figure, the relaxation results in the distortions of atomic positions for both Ni and C atoms in the contact regions.

The calculated *I-V* curves for the soldered configuration (Fig. 1, top panel) for symmetric bias configuration are shown in Fig. 2. For comparison purposes we have also included, in the same figure, the corresponding *I-V* curves for the nonsoldered case (Fig. 1, bottom panel). The inset shows the transmission function, $T(E)$, for the two cases. As can be seen in the figure, the soldered tube shows a reduction in the current and also a reduction in the Ohmic character when compared to the nonsoldered case. These can be attributed to the scattering in the soldered region. The transmission function shows an increase in the gap region (see inset).

We next turn our attention to soldered multiterminal SWCN junctions. In particular, the three-terminal junctions are useful in that they can be used in device applications in which the third terminal can be used for controlling the switching mechanism, power gain, or other transisting applications that are needed in any extended molecular electronic circuit. Experimental works have reported the existence of rectification properties in SWCN *Y* junctions.[18,19] The experimental findings were supported by our theoretical calculations, which demonstrated that *Y* junctions made of SWCN and having all their branches of finite lengths exhibit ballistic rectification and switching properties for various bias configurations.[20–22] Here we extend our calculations for three-terminal SWCN junctions obtained using soldering of individual SWCNs.

In Fig. 3 we show fully relaxed geometries of a (8,0)-(8,8)-(8,0) SWCN *Y* junction and a (10,10)-(18,0)-(10,10) SWCN *T* junction created by soldering three SWCN branches by Ni clusters. All outer ends of each of the three arms of the *T* and *Y* junctions are taken to be in contact with the transition-metal leads consisting of Ni atoms (not shown).

The *I-V* curves obtained for the *Y* junction in Fig. 3 are shown in Fig. 4. The current directions and the voltages on the three arms are indicated in the upper inset. The main

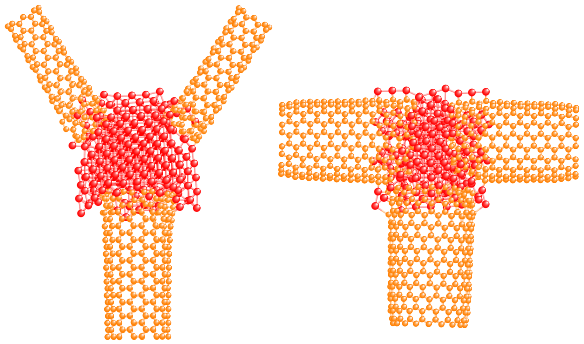

FIG. 3. (Color online) Fully relaxed geometries of two soldered multiterminal junctions made of three SWCN pieces soldered in the middle by a Ni cluster. The soldering in the right leads to a (10,10)-(18,0)-(10,10) SWCN *T* junction, while the soldering in the left leads to an (8,0)-(8,8)-(8,0) SWCN *Y* junction.

graph shows the calculated currents in the three arms of the *soldered Y* junction as a function of the bias voltage V_3. The voltage configuration for this plot has been set to $V_1=V_2=0.0$ V. This setup makes the *Y* junction a two-terminal device for the investigation of rectifying behavior. As seen in the figure, there is a noticeable increase in the current for positive values of the bias voltage V_3, while for negative values of V_3 the current is negligible. The *I-V* characteristics, thus, display a distinct asymmetry and rectifying behavior. While this behavior is similar to the *nonsoldered* case, although with significantly lower values of the current (lower inset), a striking difference can be observed. The rectification direction for the soldered *Y* junction appears to undergo a reversal about $V_3=0$.

While the *T* junction in Fig. 3 was created by soldering three SWCNs, it is also possible to create such junctions by soldering two SWCNs as shown in Fig. 5. This structure is

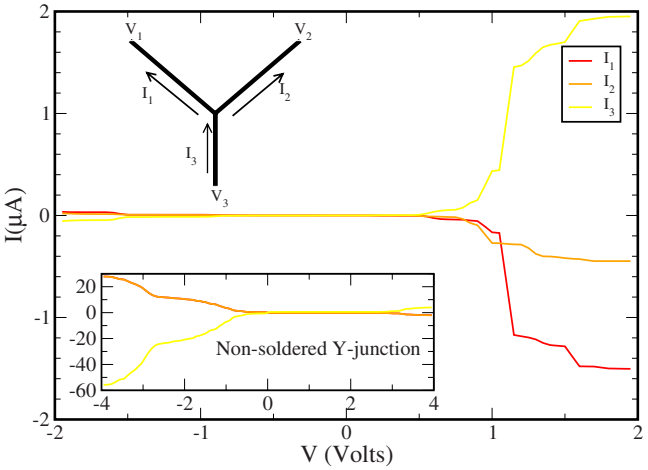

FIG. 4. (Color online) The *I-V* curves obtained for the soldered *Y* junction in Fig. 3 (left). The current directions and the voltages on the three arms are indicated in the upper inset. The main graph shows the calculated currents in the three arms of the *soldered Y* junction as a function of the bias voltage V_3. The voltage configuration for this plot has been set to $V_1=V_2=0.0$ V. The *I-V* characteristics show asymmetry and rectification. The corresponding *I-V* curves for the nonsoldered *Y* junction are shown in the lower inset.

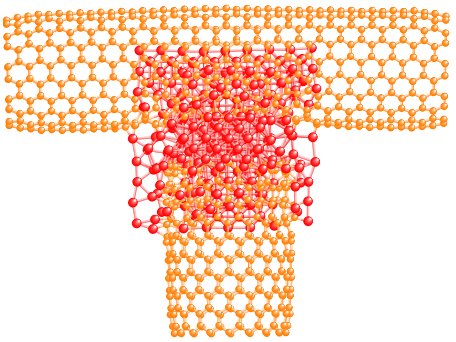

FIG. 5. (Color online) Fully relaxed geometry of a (10,10)-(18,0)-(10,10) junction obtained by soldering one end of a (18,0) SWCN with the middle of a straight (10,10) SWCN with the help of a Ni cluster.

obtained by soldering one end of a (18,0) SWCN into the middle of a (10,10) SWCN with a Ni cluster. The (10,10)-(18,0)-(10,10) *T* junction thus obtained and shown in Fig. 5 is fully relaxed using molecular-dynamics simulations. The calculated transmission functions, $T(E)$, of the two *T* junctions in Figs. 3 and 5 are shown in Fig. 6. It is apparent from this figure that the two $T(E)$'s have similar energy dependence despite the fact that they have entirely different soldering configurations. Both junctions display good transmission along the horizontal branches $[T_{LR}(E)]$. This is rather surprising since, unlike in Fig. 3, the horizontal arms of the *T* junction in Fig. 5 are not entirely separated by soldering material. Furthermore, the two *T* junctions display poor transmission between left-central $[T_{LC}(E)]$ and right-central $[T_{RC}(E)]$ branches. The similarity in the $T(E)$ functions suggests similarity in their transport properties of the two *T* junctions. This indeed is the case as demonstrated in Fig. 7,

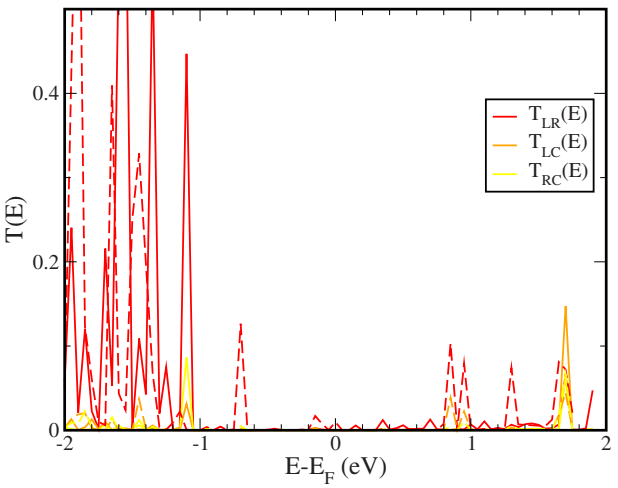

FIG. 6. (Color online) Transmission coefficients $T(E)$ for the *T* junctions shown in Fig. 3 (right, solid curves) and Fig. 5 (dashed curves).

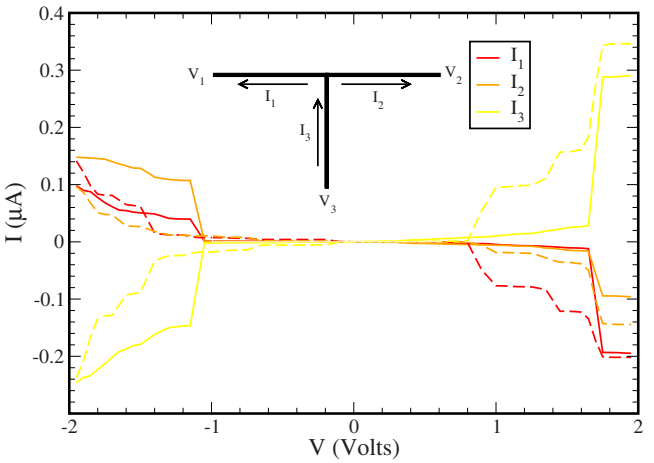

FIG. 7. (Color online) *I-V* characteristics for the *T* junctions shown in Fig. 3 (right, solid curves) and Fig. 5 (dashed curves).

where we plot the *I-V* curves for these tubes obtained under the V_3 bias and the bias configuration $V_1=V_2=0.0$ V. It is apparent that the two *T* junctions cannot rectify in either direction. Additionally, it should be noted that the values of the electronic currents through the soldered junctions are one order of magnitude smaller compared with the corresponding values in the case of the nonsoldered junctions.

While our results indicate that soldering of multibranched SWCNs in the form of *T* or *Y* SWCNs fails to reproduce the transport properties of the corresponding nonsoldered junctions in general, they, however, confirm another important feature: Namely, they demonstrate that the rectifying and switching properties of the *Y* and *T* junctions are neither the result only of the bias configuration nor the characteristics of the contacts between the tubes and the metallic leads. Because if they were so, soldering could not have such a dramatic effect on the rectification properties. The present results demonstrate that the transport properties of the *Y* and *T* junctions are strongly dependent on their inherent properties as previously demonstrated in our earlier works for the nonsoldered junctions.[20–22] This inherent characteristic depends on the symmetry of the "spacer" region[21] (i.e., the region that joins the three branches) and the way this is bonded to the branches. In the absence of this inherent characteristic, the spacer of the soldered junctions reduces the transport pathways which deviate from the straight trajectories.

In conclusion, soldering appears to reduce the current as well as the Ohmic character. More importantly, for multiterminal SWCN junctions, soldering can significantly alter the rectification properties, even reversing its direction due to the destruction of the symmetry of the junction's spacer region.

ACKNOWLEDGMENTS

The present work is supported by U.S.-ARO (Grant No. W911NF-05–1-0372) and DOE (Grants No. DE-FG02–00ER45817 and No. DE-FG02–07ER46375).

*andriot@iesl.forth.gr
†super250@pop.uky.edu

[1] H. Tanaka, S. Akita, L. Pan, and Y. Nakayama, Jpn. J. Appl. Phys., Part 1 **43**, 1651 (2004).
[2] R. C. Smith, D. C. Cox, and S. R. P. Silva, Appl. Phys. Lett. **87**, 103112 (2005).
[3] M. S. Wang, J. Y. Wang, and L.-M. Peng, Appl. Phys. Lett. **88**, 243108 (2006).
[4] K. Asaka, H. Nakahara, and Y. Saito, Appl. Phys. Lett. **92**, 023114 (2008).
[5] P. Rai-Choudhury, *Handbook of Microlithography* (SPIE, Washington, 1997), Vol. 1.
[6] C. O. Girit and A. Zettl, Appl. Phys. Lett. **91**, 193512 (2007).
[7] S. Datta, *Electronic Transport in Mesoscopic Systems* (Cambridge Univ. Press, Cambridge, 1995).
[8] Y. Xue and M. A. Ratner, Phys. Rev. B **70**, 205416 (2004).
[9] Y. Xue and M. A. Ratner, Phys. Rev. B **69**, 161402(R) (2004).
[10] H. W. C. Postma, M. de Jonge, Z. Yao, and C. Dekker, Phys. Rev. B **62**, R10653 (2000).
[11] P. S. Damle, A. W. Ghosh, and S. Datta, Phys. Rev. B **64**, 201403(R) (2001).
[12] M. P. Anantram and T. R. Govindan, Phys. Rev. B **58**, 4882 (1998).
[13] A. N. Andriotis and M. Menon, Phys. Rev. B **76**, 045412 (2007).
[14] A. N. Andriotis, M. Menon, G. Froudakis, and J. E. Lowther, Chem. Phys. Lett. **301**, 503 (1999).
[15] A. N. Andriotis and M. Menon, J. Chem. Phys. **115**, 2737 (2001).
[16] A. N. Andriotis, Europhys. Lett. **17**, 349 (1992).
[17] A. N. Andriotis and M. Menon, Phys. Rev. B **57**, 10069 (1998).
[18] C. Papadopoulos, A. Rakitin, J. Li, A. S. Vedeneev, and J. M. Xu, Phys. Rev. Lett. **85**, 3476 (2000).
[19] B. C. Satishkumar, P. J. Thomas, A. Govindraj, and C. N. R. Rao, Appl. Phys. Lett. **77**, 2530 (2000).
[20] A. N. Andriotis, M. Menon, D. Srivastava, and L. Chernozatonskii, Phys. Rev. Lett. **87**, 066802 (2001).
[21] A. N. Andriotis, M. Menon, D. Srivastava, and L. Chernozatonskii, Phys. Rev. B **65**, 165416 (2002).
[22] A. N. Andriotis, D. Srivastava, and M. Menon, Appl. Phys. Lett. **83**, 1674 (2003).